WARSAW UNIVERSITY OF TECHNOLOGY Index 351733
FACULTY OF CIVIL ENGINEERING
COMMITTEE FOR CIVIL AND WATER ENGINEERING
POLISH ACADEMY OF SCIENCES ISSN 1230-2945

DOI: 10.24425/ace.2026.1401

ARCHIVES OF CIVIL ENGINEERING

Vol. LXXII ISSUE 3 2026

pp. 417 –430

Research paper

The analysis of structural characteristics distribution and compressive strength of asphalt mixture SMA-13 in two compaction methods

Yan Li[1], Zhigang Zhou[2], Shuaishuai Li[3], Shihui Guo[4]

Abstract: In order to study the influence of different compaction methods on void structural characteristics distribution and compressive strength of SMA-13 asphalt mixture, Marshall compaction instrument and rotary compaction instrument were used in the laboratory to make SMA-13 asphalt mixture specimens with different air voids. CT scanning and image processing were used to extract and compare the changes in parameters such as voids ratio, the number of voids, average equivalent diameter of voids, and void contour fractal dimension of various types of specimens. The compressive strength of various types of SMA-13 asphalt mixture specimens was obtained by uniaxial compression test and triaxial compression test. The results show that the variability of voids ratio, the number of voids, average equivalent diameter of voids, and void contour fractal dimension along the layer of SMA-13 specimens formed by rotary compaction is greater than that of specimens formed by Marshall compaction. The mean value of the number of voids, the mean value of average equivalent diameter of voids and the mean value of void contour fractal dimension of SMA-13 asphalt mixture specimens formed by two compaction methods increase with the increase of air voids. The mean value of the number of voids and the mean value of average equivalent diameter of voids of the specimens formed by Marshall compaction are larger than those of the specimens formed by rotary compaction, and the mean value of void contour fractal dimension of the specimens formed by rotary compaction is larger than that of the specimens formed by Marshall compaction when the air voids is similar. The uniaxial compressive strength and triaxial compressive strength of SMA-13 asphalt mixture under two compaction methods decrease with the increase of the mean value of the number of voids, the mean value of average equivalent diameter of voids and the mean value of void contour fractal dimension.

Keywords: asphalt mixtures, compaction method, compressive strength, void structure characteristics, road engineering, SMA-13

[1]PhD., 1) School of Civil Engineering, Nanyang Institute of Technology, Nanyang 473004, China, 2) Henan International Joint Laboratory of Dynamics of Impact and Disaster of Engineering Structures, Nanyang Institute of Technology, Nanyang 473004, China, e-mail: prettyboy86@163.com, ORCID: 0009-0000-1741-5825
[2]PhD., School of Traffic Transportation Engineering, Changsha University of Science and Technology, Changsha 410004, China, e-mail: 250430381@qq.com, ORCID: 0009-0008-0674-3899
[3]MSc., School of Traffic Transportation Engineering, Changsha University of Science and Technology, Changsha 410004, China, e-mail: 1071003260@qq.com, ORCID: 0009-0009-8691-8931
[4]PhD., 1) School of Civil Engineering, Nanyang Institute of Technology, Nanyang 473004, China, 2) Henan International Joint Laboratory of Dynamics of Impact and Disaster of Engineering Structures, Nanyang Institute of Technology, Nanyang 473004, China, e-mail: 2951528075@qq.com, ORCID: 0009-0003-5975-1597

1. Introduction

Different grading types, binder contetnt and compaction methods will cause different void structure in asphalt mixture, resulting in different road performance. At present, the laboratory compaction methods of asphalt mixture are mainly Marshall compaction and gyratory compaction. The asphalt mixture was compacted by compacting hammer impact by Marshall compaction molding, which will cause damage to the internal structure of the mixture. When the compaction work is large, the aggregate will be broken. The asphalt mixture was compacted through kneading action by gyratory compaction molding. which is close to the effect of tire rolling. Therefore, even if the asphalt mixture with the same grading and material is used, its void structure will be different under different compaction methods, so it is of great significance to study the void structure characteristics and mechanical properties of asphalt mixture under different molding methods [1].

Using CT scanning technology combined with image processing technology to study the void structure characteristics of asphalt mixture is a research method widely used by researchers at home and abroad in recent years [2–6]. The existing research on asphalt mixture is to extract the mesoscopic features of asphalt mixture specimens by CT scanning, analyze the distribution characteristics of void structure [7–13], analyze the complexity of the inner wall of the three-dimensional void in asphalt mixture by using the fractal dimension of void profile in fractal theory [14–18], and analyze its road performance in combination with mechanical indexes such as split strength [19, 20]. However, there are few studies on the void structure distribution characteristics and mechanical properties of SMA-13 asphalt mixture with the same material and the same gradation under different compaction methods. Because the void structure distribution of asphalt mixture will directly affect its mechanical properties, this paper applies two molding methods of Marshall compaction molding and gyratory compaction molding to prepare SMA-13 asphalt mixture specimens with different air void. The void structure parameters of the specimens are obtained and compared by CT tomography, and the best compaction method of asphalt mixture is verified by combining the compressive strength index.

2. Specimen preparation of SMA-13 asphalt mixture

2.1. Testing material

Stone mastic asphalt SMA-13 was used in the test. The coarse aggregate is basalt, the fine aggregate is limestone, the kind of mineral powder is limestone, the bitumen is SBSI-D modified bitumen, and the fiber is lignified fiber.

According to the SMA-13 aggregate gradation table in the Technical Specifications for Construction of Highway Asphalt Pavement [21], the asphalt mixture aggregate gradation used in this test is designed as Table 1 and Fig. 1.

Table 1. The aggregate design gradation of SMA-13 asphalt mixture

Gradation	Size of screen mesh (mm)	The percentage of weight of aggregate through the following sieve (%)									
		16	13.2	9.5	4.75	2.36	1.18	0.6	0.3	0.15	0.075
SMA-13	Upper limit of gradation	100.0	100.0	75.0	34.0	26.0	24.0	20.0	16.0	15.0	12.0
	Lower limit of grading	100.0	90.0	50.0	20.0	15.0	14.0	12.0	10.0	9.0	8.0
	Composite gradation	100.0	92.3	66.2	27.2	19.5	17.0	14.4	12.6	11.4	9.5

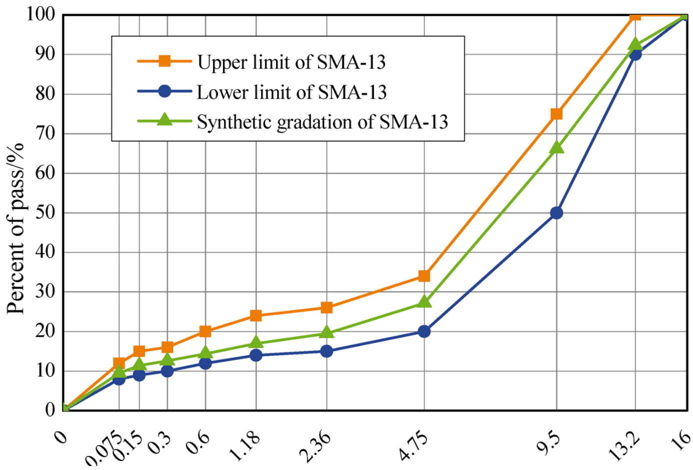

Fig. 1. Gradation curve of mineral aggregate of SMA-13

Using the aggregates above to combine design, Marshall test is conducted to determine the optimal binder content. The optimal bitumen-aggregate ratio is determined to be 5.9% through tests. The bituminous binder content is 5.6%. The Marshall stability test results of SMA-13 are presented in Table 2.

Table 2. Marshall stability test results of SMA-13

Binder-stone ratio (%)	Bulk density (g/cm3)	Percent air voids in bituminous mixtures VV (%)	Voids filled with asphalt VFA (%)	Voids in mineral aggregate VMA (%)	Marshall stability MS (kN)	Flow value FL (0.1 mm)	Bulk density of the mineral aggregate (g/cm3)
5.9	2.487	4.3	75	17.2	8.6	3.4	2.708

2.2. Specimen preparation

Two compaction methods of Marshall compaction molding and rotary compaction molding were used to prepare SMA-13 asphalt mixture specimens. The corresponding compaction times (single side) for asphalt mixture specimens formed by Marshall compaction molding with air voids content of about 4%, 6%, 8%, and 10% are 75 times, 40 times, 20 times, and 10 times respectively using the standard compaction method [22]. The specimens formed by rotary compaction molding with air voids content of about 4%, 6%, 8% and 10%, the number of rotary compaction is 25 times, 10 times, 5 times and 3 times, respectively.

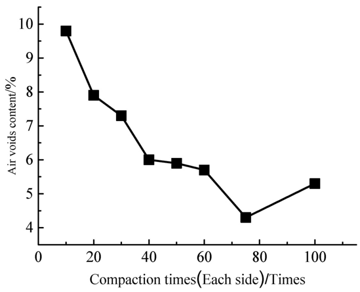

Fig. 2. Relationship between air voids content and compaction times of SMA-13

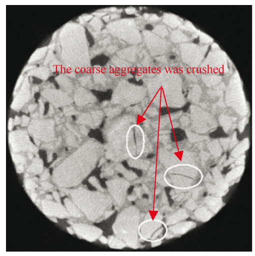

Fig. 3. The CT scan image of SMA-13 asphalt mixture compacted 100 times

From Fig. 2, it can be seen that for asphalt mixture specimens formed by Marshall compaction molding, the air voids content gradually decreases with the increase of compaction times, and the air voids content is the smallest at 75 compaction times. There is a slight increase in air voids content at 100 compaction times, which is due to the continued increase in compaction work causing some coarse aggregates to be crushed, resulting in new cracks that are not wrapped by bitumen as shown in Fig. 3.

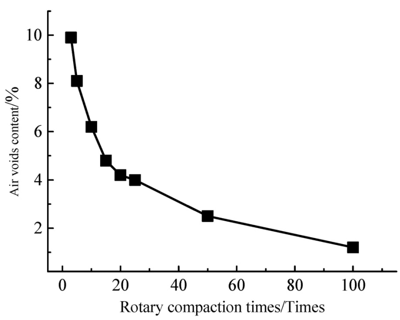

Fig. 4. Relationship between air voids content and rotary compaction times of SMA-13

From Figs. 2 and 4, it can be seen that for SMA-13 asphalt mixture, as the number of rotational compaction increases, the air voids content of the specimen gradually decreases, but the rate of air voids content reduction gradually slows down. From the perspective of air voids content alone, the compaction work with rotary compaction 25 times is equivalent to the compaction work with Marshall standard compaction 75 times, indicating that the rotary compaction effect is better than the Marshall compaction effect.

3. CT scanning and image processing

In this paper, the asphalt mixture specimens are scanned by the multi-slice spiral CT scanning test machine, and the linear array CT scanning mode is used for scanning. The scanning thickness of each CT image is 1mm, and the CT scanning of cross section is conducted at an interval of 5 mm along the height direction of the test piece. The voltage of CT machine is 310 kV and the current is 2.55 mA, the resolution was 0.2 × 0.2 mm, the CT scanning speed was about 3 minutes per section. The acquired CT image is processed with MATLAB software, and the examples of processing results are shown in Fig. 5 and Fig. 6.

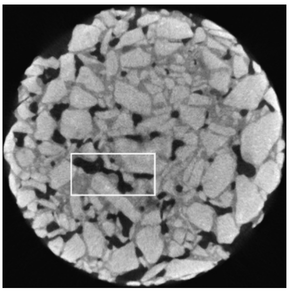

Fig. 5. CT scan image of SMA-13

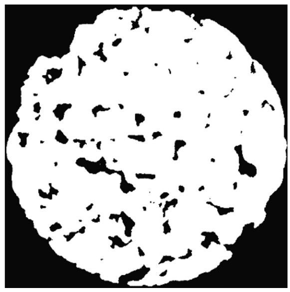

Fig. 6. Processed CT image of SMA-13

4. Characterization parameters of pore microstructure

The micro-structural characteristics such as the number, size, shape, distribution and connectivity of voids in asphalt mixture affect the mechanical strength and permeability of asphalt mixture. Because the shape of the void structure is very irregular, it needs to be corrected [6]. The void characteristic parameters selected in this paper are voids ratio, the number of voids, the average equivalent diameter of voids and void contour fractal dimension.

The void ratio of each cross-section refers to the ratio of the void area within the cross-section to the total cross-sectional area, and the void ratio of the entire specimen is the average of the void ratios of all cross- sections. The number of voids is the sum of the number of voids in all sections of the specimen. The calculation formula of void average equivalent diameter is shown in Eq. (4.1).

$$d = 2 \times \sqrt{\frac{\sum_{i=1}^{n} A_i}{N_i \pi}} \tag{4.1}$$

where Ai is the area of the i−th void in the CT image, and Ni is the number of viods.

(a) (b)

Fig. 7. The CT image of local void in SMA -13 asphalt mixture

Fig. 7a shows the enlarged shape of a local position (within the white rectangular box in Fig. 5) in the cross-sectional CT image of a certain specimen. The black part represents the voids in Fig. 7b after processing with digital image processing technology. Obviously, the measurement value of the viods contour will have a significant difference depending on the length of the ruler used. The shorter the ruler, the longer the measurement value of the gap contour. According to fractal theory, the relationship between the void contour length L and the scale length ε is shown in Eq. (4.2).

$$L = k\varepsilon^{1-D} \tag{4.2}$$

k is a constant related to scale in the Eq. (4.2), Eq. (4.3) can be obtained by taking logarithms on both sides of Eq. (4.2).

$$\lg L = (1 - D)\lg \varepsilon + \lg k \tag{4.3}$$

Using a set of scales with different lengths to measure the contour length, and then a straight line with slope $k = 1 - D$ can be obtained through linear regression in double logarithmic coordinates, so the fractal dimension of the void contour is $D = 1 - k$.

In this paper, the Image-Pro Plus software is used to extract the voids feature parameters of the scanned and processed CT images, as shown in Fig. 8.

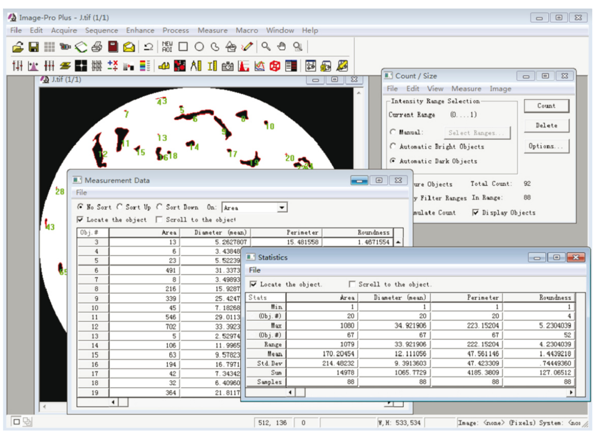

Fig. 8. Extraction process of micro-structural characteristics of voids by applying Image-Pro Plus software

5. Analysis of internal void characteristics of SMA-13 asphalt mixture

5.1. Analysis of void characteristics of SMA-13 under different compaction work

(1) Analysis of void structure characteristics of SMA-13 asphalt mixture formed by Marshall compaction

The distribution of voids ratio, the number of voids, the average equivalent diameter of voids and void contour fractal dimension along the height of the SMA-13 asphalt mixture specimens formed by Marshall compaction with the air viods content of 4.2%, 5.8%, 8.0% and 9.6% respectively under different compaction work are shown in Figs. 9– 12.

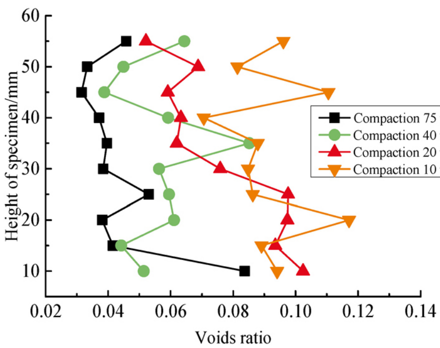

Fig. 9. Distribution of voids ratio along the height of specimen

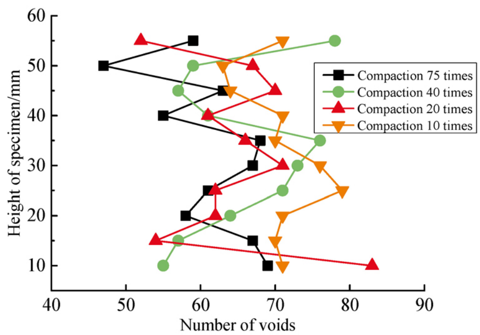

Fig. 10. Distribution of the number of voids along the height of specimen

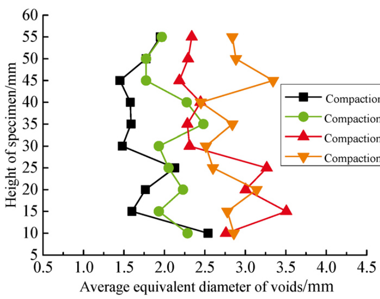

Fig. 11. Distribution of average equivalent diameter of voids along the height of specimen

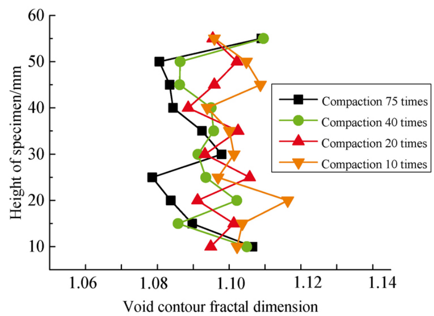

Fig. 12. Distribution of void contour fractal dimension along the height of specimen

As can be seen from Figs. 9– 12, the voids ratio along the height of the specimen shows the characteristics of first decreasing, then increasing and then decreasing, but the lower end of the voids ratio is larger than the upper end with the increase of compaction times for SMA-13 asphalt mixture specimen formed by Marshall compaction. The number of voids decreases gradually with the increase of compaction times, and is more evenly distributed along the horizon layers. The fluctuation of the number of voids at both ends of the specimen is larger than that at the middle part. The average equivalent diameter of voids decreases gradually with the increase of compaction times. The void contour fractal dimension at both ends of the specimen changes significantly, while the change in the middle part is relatively small. This is because the compaction work is transmitted from both ends to the middle, and the impact on the middle part is relatively small under double-sided compaction. In addition, the void contour fractal dimension decreases with the increase of the compaction times.

(2) Analysis of void structure characteristics of SMA-13 asphalt mixture formed by gyratory compaction

The distribution of voids ratio, the number of voids, the average equivalent diameter of voids and void contour fractal dimension along the height of the SMA-13 asphalt mixture specimens formed by gyratory compaction with the air voids content of 3.8%, 5.7%, 7.9% and 9.8% respectively under different compaction work are shown in Figs. 13–16.

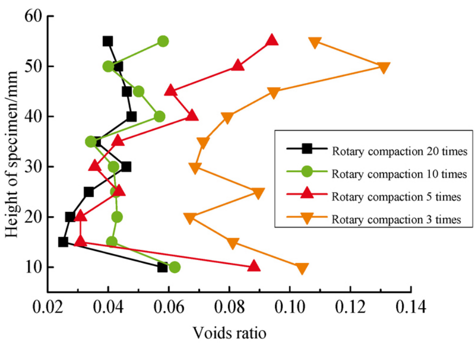

Fig. 13. Distribution of voids ratio along the height of specimen

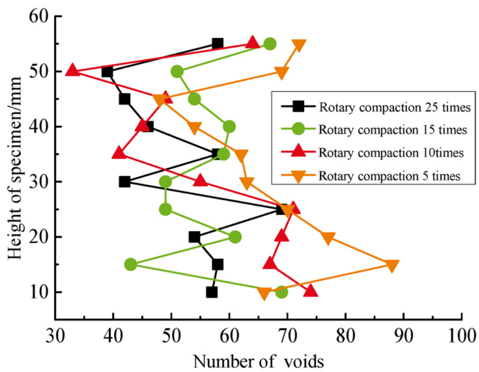

Fig. 14. Distribution of number of voids along the height of specimen

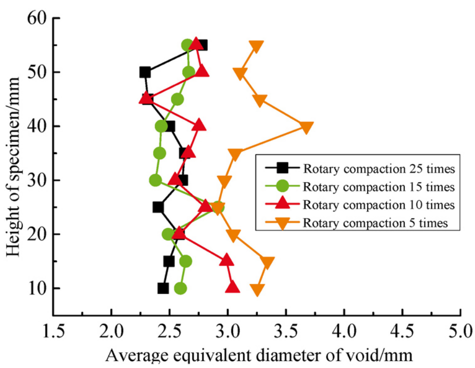

Fig. 15. Distribution of average equivalent diameter of voids along the height of specimen

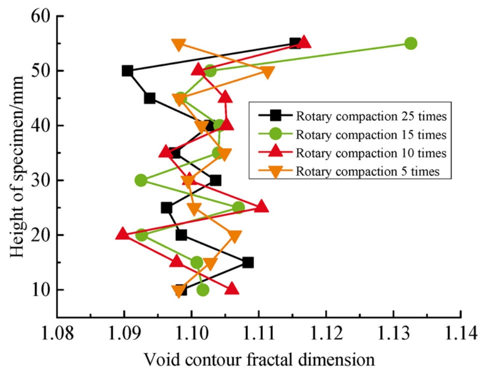

Fig. 16. Distribution of number of voids along the height of specimen

It can be seen from Figs. 13–16 that as the compaction work increases, the voids ratio decreases and the distribution along the layers becomes more uniform. The variability of the number of viods along the stratigraphic distribution is significant. The average equivalent diameter of voids is evenly distributed along the layers. The void contour fractal dimension is relatively evenly distributed along the layers, and there is significant variability in the upper part of the specimen.

5.2. Analysis of void characteristics of SMA-13 with different compaction methods

In order to compare the influence of Marshall compaction and gyratory compaction on the void structure of SMA-13 asphalt mixture, the specimens formed by Marshall compaction with air viods of 5.8% and the specimens formed by gyratory compaction with air viods of 5.7% were selected for comparison. The distribution of each void parameter is shown in Figs. 17–20.

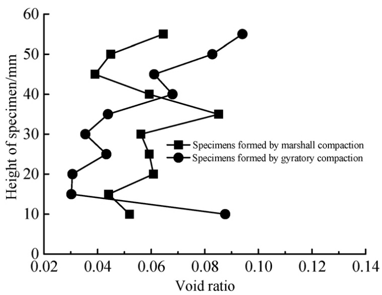

Fig. 17. Distribution of void ratio along the height of specimen

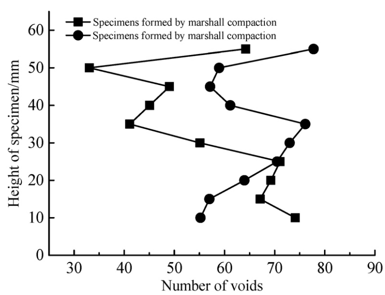

Fig. 18. Distribution of the number of voids along the height of specimen

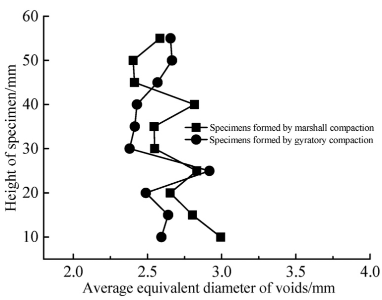

Fig. 19. Distribution of average equivalent diameter of voids along the height of specimen

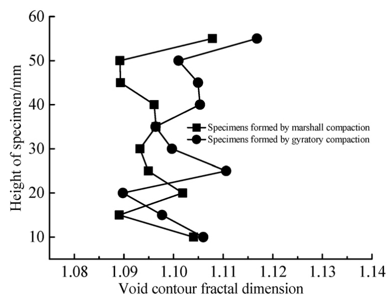

Fig. 20. Distribution of void contour fractal dimension along the height of specimen

It can be seen from Figs. 17–20 that for SMA-13 asphalt mixture specimens with similar air voids content, the number of voids in each layer of the specimens formed by Marshall compaction is higher than that of the specimens formed by rotary compaction. The average equivalent diameter of voids in the specimens formed by Marshall compaction is slightly larger than that of the specimens formed by rotary compaction, while the void contour fractal dimension of the specimens formed by Marshall compaction is smaller than that of the specimens formed by rotary compaction.

The fluctuation of viods ratio distribution along the height of specimens formed by Marshall compaction is greater than that of specimens formed by rotary compaction. The regularity of the distribution of the number of voids along the height of specimen formed by rotary compaction is better than that of formed by Marshall compaction. The average equivalent diameter of voids and void contour fractal dimension along the layer is relatively similar under the two compaction methods. The variability of viods ratio, the number of voids, average equivalent diameter of voids and void contour fractal dimension along the layer of specimens formed by rotary compaction is greater than that of specimens formed by Marshall compaction. This is because during the rotary compaction process, the degree of reconstruction of the aggregate is much greater than that of Marshall compaction, and the variability of the void structure is greater than that of Marshall compaction.

6. Comparison of compressive strength of SMA-13 specimens under two compaction methods

The height of the specimen used in this study is about 63.5 mm, and the diameter is about 100 mm. The uniaxial compression and triaxial compression tests are carried out on the specimens with different air viods in normal temperature. The confining pressure for the triaxial compression test is 0.3 MPa and the loading rate is 2 mm/min.

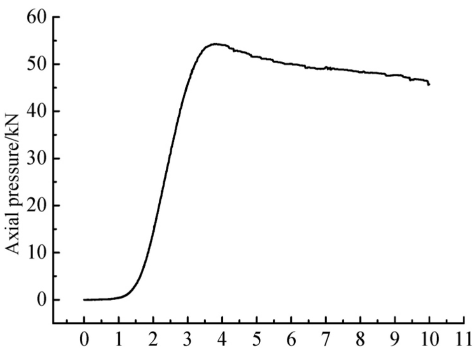

Fig. 21. The uniaxial compression test for SMA-13

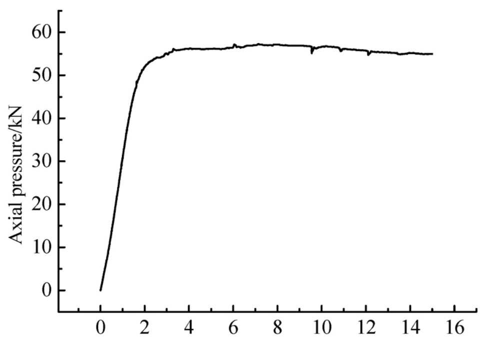

Fig. 22. The triaxial compression test for SMA-13

For the uniaxial compression test, if the axial pressure reaches the peak value and continues to be loaded, the axial pressure will gradually decrease as shown in Fig. 21. During the triaxial compression test, it was found that for different types of speciments, when the maximum axial displacement reached 10 mm and the axial pressure continued to increase, the axial pressure remained basically unchanged, and some decreased slightly as shown in Fig. 22.

Excessive deformation can also be defined as failure [16]. Therefore, for triaxial test, the axial displacement of 10 mm is used as the test termination condition, that is, the strength with axial strain of 15.4% is triaxial compressive strength.

Based on the compressive strength of SMA-13 asphalt mixture obtained from experiments and combined with the void structure characteristics of voids, the influence of the characteristics of void structure on the mechanical properties of SMA-13 asphalt mixture is analyzed.

It can be seen from Fig. 23 that the mean value of the number of voids in SMA-13 asphalt mixture specimens increases with the increase of air voids content, while the uniaxial compressive strength and triaxial compressive strength decrease with the increase of the mean value of number of voids under two compaction methods. The mean value of the number of voids in the specimens formed by Marshall compaction is greater than that formed by rotary compaction under the condition of similar air voids, indicating that the number of voids formed inside specimens formed by Marshall compaction method is greater.

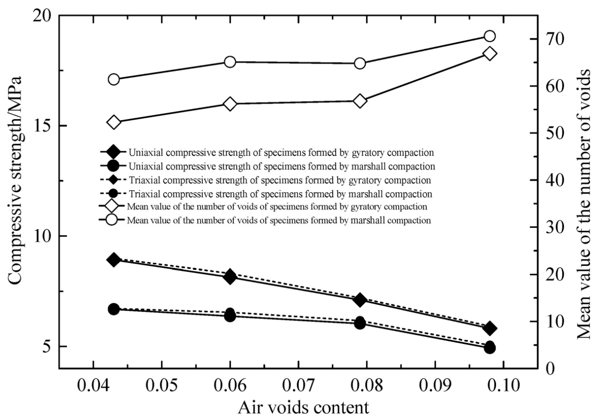

Fig. 23. Relationship between compressive strength, mean value of the number of voids and air voids content

It can be seen from Fig. 24 that the mean value of average equivalent diameter of voids in SMA-13 asphalt mixture specimens increases with the increase of air voids content, while the uniaxial compressive strength and triaxial compressive strength decrease with the increase of the mean value of average equivalent diameter of voids under two compaction methods. The mean value of average equivalent diameter of voids in the specimens formed by Marshall compaction is greater than that formed by rotary compaction under the condition of similar air voids, indicating that the void size formed inside specimens formed by Marshall compaction method is larger.

It can be seen from Fig. 25 that the mean value of void contour fractal dimension in SMA-13 asphalt mixture specimens increases with the increase of air voids content, while the uniaxial compressive strength and triaxial compressive strength decrease with the increase of the void contour fractal dimension under two compaction methods. The mean value of void contour fractal dimension in the specimens formed by rotary compaction is greater than that formed by Marshall compaction under the condition of similar voids content, indicating that the complexity of void structure inside specimens formed by rotary compaction is higher.

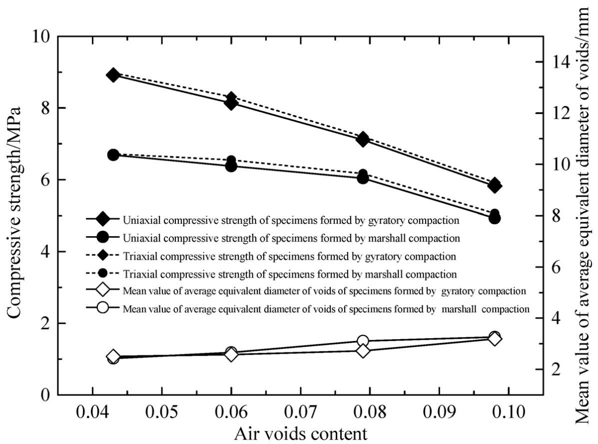

Fig. 24. Relationship between compressive strength, mean value of average equivalent diameter of voids and air voids content

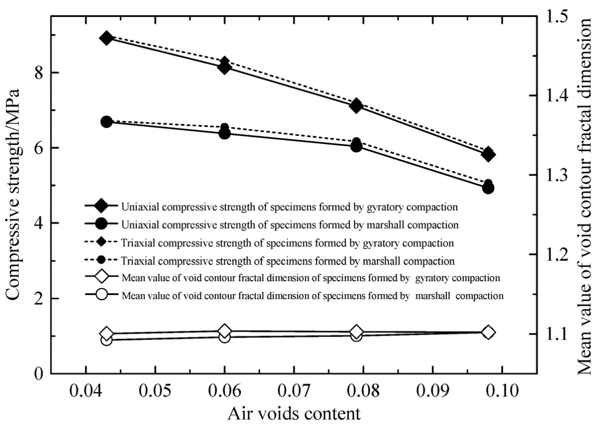

Fig. 25. Relationship between compressive strength, mean value of void contour fractal dimension and air voids content

7. Conclusions

In this paper, the changes of void structure characteristics and compressive strength of SMA-13 asphalt mixture under different compaction methods and compaction work are compared and studied, the conclusions are as follows:

(1) The distribution of void ratio inside the specimen of SMA-13 asphalt mixture formed by Marshall compaction is approximately symmetrical along the height direction of the specimen. The distribution of void ratio inside the specimen of SMA-13 asphalt mixture formed by gyratory compaction shows a trend of large at both ends and small in the middle. The mean value of the number of voids and the mean value of average equivalent diameter of voids of the

specimens formed by Marshall compaction are larger than those of the specimens formed by rotary compaction, the mean value of void contour fractal dimension of the specimens formed by rotary compaction is larger than that of the specimens formed by Marshall compaction when the air voids content is similar.

(2) The uniaxial compressive strength and triaxial compressive strength of SMA-13 asphalt mixture under two compaction methods decrease with the increase of the mean value of the number of voids, the mean value of average equivalent diameter of voids and the mean value of void contour fractal dimension.

The research results can provide theoretical guidance for improving compaction instruments and construction processes, and enhancing the service life of asphalt pavement. In subsequent research, core sampling will be conducted from the asphalt pavement construction site to analyze the differences in void structure characteristics and compressive strength of asphalt mixture specimens formed in laboratory and on-site, in order to determine whether to use rotary compaction method to evaluate the road performance of asphalt pavement.

Acknowledgments

This work was supported by the National Natural Science Foundation of China (no. 51878079), the Cross Project in Nanyang Institute of Technology (no. 520008), Doctoral Research Project of Nanyang Institute of Technology (no. 510128), Nanyang Science and Technology t Program (no. 24KJGG076).

References

[1] L.P. Li and F. Zhang, "Comparative analysis of warm mix asphalt Mar-shall and gyratory compaction densification curve", *Highway Engineering*, vol. 40, no. 1, pp. 29–32+47, 2015.

[2] X.N. Zhang, "Basic methods of digital image technology for material structure of asphalt mixtures", *Journal of South China University of Technology: Natural Science Edition*, vol. 40, no. 10, pp. 166–173, 2012.

[3] Y. Zhang, W.C. Wang, L. Fang, J.Z. Liu, C.Y. Xiao, and B. Yu, "Assessment of air void distribution of rutted asphalt mixtures using X-ray CT technology", *Journal of Beijing University of Technology*, vol. 50, no. 4, pp. 508–522, 2024.

[4] Y.B. Xie, J. Ren, T.L. Zhu, J.Z. Zhao, Y. Yao, and Y. Ren, "Characterization of voids in asphalt mixtures with different grading methods and different grading types", *Shanghai Highways*, no. 1, pp. 91–96+121–122, 2021.

[5] H.Z. Zhu, Q.Q. Tan, S.P. Fan, and G.Q. Wan, "Research progress of bituminous mixture mesostructure based on image technology", *Journal of Chongqing Jiaotong University (Natural Science)*, vol. 40, no. 10, pp. 97–110, 2021.

[6] S.Y. Chen, Z.P. You, S.L, Yang, A. Garcia, and L. Rose, "Influence of air void structures on the coefficient of permeability of asphalt mixtures", *Powder Technology*, vol. 377, pp. 1–9, 2021, doi: 10.1016/j.powtec.2020.08.082.

[7] J.B. Król, R. Khan, and A.C. Collop, "The study of the effect of internal structure on permeability of porous asphalt", *Road Materials and Pavement Design*, vol. 19, no. 4, pp. 935–951, 2017, doi: 10.1080/14680629.2017.1283355.

[8] J. Xu, D.Y. Ren, Z. Li, and X.Y. Li, "Investigation on mesoscopic pore characteristics in asphalt mixtures under varied compaction levels based on CT technology", *Journal of Changsha University of Science & Technology (Natural Science)*, vol. 21, no. 1, pp. 12–21, 2024, doi: 10.19951/j.cnki.1672-9331.20231215001.

[9] H.N. Wang, L. Li, and Z.P. You, "Characterization on the 3D air void spatial distribution based on the microstructure of asphalt mixture", *Journal of Wuhan University of Technology*, vol. 34, no. 8, pp. 61–67, 2012.

[10] F. Yi, Y. Jin, and J. Su, "Mesoscopic analysis of air void distribution of asphalt mixture in two compaction methods", *Journal of Highway and Transportation Research and Development*, vol. 31, no. 3, pp. 26–31, 2014.

[11] H.N. Yu et al., "Review of digital twin model of asphalt mixture performance based on mesostructure characteristics", *China Journal of Highway and Transport*, vol. 36, no. 3, pp. 20–44, 2023, doi: 10.19721/j.cnki.1001-7372.2023.03.002.

[12] E. Masad, V.K. Jandhyala, N. Dasgupta, N. Somadevan, and N. Shashidhar, "Characterization of air void distribution in asphalt mixes using X-ray computed tomography", *Journal of Materials in Civil Engineering*, vol. 14, no. 2, pp. 122–129, 2002, doi: 10.1061/(ASCE)0899-1561(2002)14:2(122).

[13] C.Q. Yan, J. Yang, N. Zuo, and L.Y. Jiao, "Study on initial void distribution of asphalt mixture", *Journal of China and Foreign Highway*, vol. 35, no. 5, pp. 296–301, 2015, doi: 10.14048/j.issn.1671-2579.2015.05.068.

[14] G. Leonardi, "Fractal dimension for the characterization of the porosity of asphalt concretes", *Archives of Civil Engineering*, vol. 56, no. 4, pp. 321–333, 2010, doi: 10.2478/v.10169-010-0018-5.

[15] F. Wang, Y. Xiao, P.D. Cui, L.T. Mo, and M.J. Fang, "Review on the characterization of aggregate morphology and its influence on asphalt mixture properties", *Materials Reports*, vol. 36, no. 17, pp. 21030063–13, 2022, doi: 10.11896/cldb.21030063.

[16] L.Y. Kong, et al., "Antiskid decay prediction of asphalt mixtures based on aggregate mechanical properties and gradation fractals", *Journal of Southeast University (English Edition)*, vol. 40, no. 1, pp. 58–67, 2024.

[17] Y.J. Lv, B. Liu, L. Zhang, and W. Tang, "Research on void characteristics and multifractal of asphalt mixture", *Journal of China and Foreign Highway*, vol. 41, no. 2, pp. 273–280, 2021, doi: 10.14048/j.issn.1671-2579.2021.02.055.

[18] F.Y. Li, A.J. Yue, and J.H. Huang, "Gradation optimization design of rubber asphalt mixture based on fractal theory", *Journal of Huaiyin Institute of Technology*, vol. 32, no. 1, pp. 57–63, 2023.

[19] T.Q. Ren, H.T. Zhang, X.Q. Zhang, and J.F. Sun, "Influence of different forming methods on road performance and meso-structure of asphalt mixture", *Forest Engineering*, vol. 38, no. 4, pp. 172–180, 2022.

[20] H. Wu, J.P. Zhang, and B.G. Wang, "Relationship between characteristic of void and road performance of porous asphalt mixture", *Journal of Traffic and Transportation Engineering*, vol. 10, no. 1, pp. 1–5, 2010, doi: 10.19818/j.cnki.1671-1637.2010.01.001.

[21] JTG F40-2004 Technical specifications for construction of highway asphalt pavement. China Communications Press, 2017.

[22] JTG E20-2011 Standard test methods of bitumen and bituminous mixtures for highway engineering. China Communications Press, 2011.

Received: 2024-09-26, Revised: 2025-02-08